UNIVERSITY *of* York

This is a repository copy of *Extending Coverage and Capacity from High Altitude Platforms With A Two-tier Cellular Architecture*.

Extending Coverage and Capacity from High Altitude Platforms With A Two-tier Cellular Architecture

Steve Chukwuebuka Arum, David Grace, and Paul Daniel Mitchell

Abstract—Conventional coverage and capacity from a high altitude platform (HAP) over an extended coverage area suffer significantly from inter-cell interference (ICI), antenna beam broadening, and uneven cell loading, which results in poor edge performance. In this paper, we show how a single antenna array on a HAP can be used to mitigate against these and achieve ubiquitous coverage by forming two tiers of a homogeneous contiguous cellular structure. We propose separate algorithms that implement the two-tier architecture with many antenna beams, which are used to form cells, and associate users with an appropriate cell and tier. A user associates with the cell and tier, which offer the best carrier power-to-noise ratio (CNR) and carrier power-to-interference-plus-noise ratio (CINR) respectively. The performance of the architecture, which is evaluated using simulation, is compared with a typical one-tier architecture. The results show that the two-tier architecture achieves over 30% higher user throughput and enhances throughput fairness and edge-of-cell connectivity by centralising as many users as possible within cells compared to the typical one-tier architecture. These benefits are better exploited by ensuring spectrum orthogonality between the two tiers.

Index Terms—High Altitude Platform, Coverage, Capacity, Cellular Architecture, Tier, Beam Pointing.

---◆---

1 INTRODUCTION AND MOTIVATION

WITH the need for ubiquitous wireless coverage and enhanced capacity, interest in using high altitude platforms (HAPs) for wireless communications is increasing considerably. This is due to reasons such as their better propagation characteristics, lower costs, and higher flexibility compared to terrestrial and satellite systems [1], [2]. A HAP, which is an aeronautic platform operating at altitudes typically between 17–22 km, can provide contiguous coverage over an extended area at a significantly lower cost than terrestrial and satellite systems. This is desirable given the vision of next generation networks to cost-effectively connect the unconnected/under-connected [3], [4]. Thus, HAPs are ideal for providing coverage in remote or rural areas with characteristically low user densities, which otherwise cannot be served cost-effectively.

A HAP communication system, like terrestrial

and satellite systems, forms beams on the ground at given elevation angles to provide both coverage and capacity to the users [5]. These beams formed simultaneously from multi-beam phased array antennas as in [6], which are used to create cells isolated by the HAP antenna radiation pattern [7], are limited by the beamforming techniques implemented. Ideally, each beam with a steep roll-off illuminates its corresponding cell, ensuring that no power is delivered outside the cell boundaries. Unfortunately, due to the imperfect roll-off of practical antenna beams, inter-cell interference (ICI) is introduced, and is worsened by the limitations of the array beamforming technique [8]. Furthermore, as the elevation angle of beams referenced at boresight [9] reduces, the resulting cell footprints broaden, thereby increasing both cell overlap [10] and ICI. These affect the achievable coverage and capacity, especially at the edge of the HAP extended coverage area. In order to avoid this, most studies on HAP cellular coverage, as highlighted in Section 2, limit the coverage area to within a 30 km radius with negligible beam broadening. In our previous work [10], we proposed a framework for delivering contiguous coverage and capacity from a HAP over an area of over 60 km radius by exploiting a phased array

- S. C. Arum is with the Applied Research, British Telecoms, Adastral Park, Martlesham Heath, Ipswich IP5 3RE. E-mail: steve.arum@bt.com
- D. Grace and P. D. Mitchell are with the Department of Electronic Engineering, University of York, Heslington, York, YO10 5DD. E-mail: {david.grace, paul.mitchell}@york.ac.uk

antenna beam-pointing algorithm, which explicitly considers beam broadening to minimise overlap.

Why Two-tier HAP Architecture. The one-tier HAP extended coverage and capacity architecture in [10], which motivates this work, has a few challenges. Firstly, with the worsening antenna efficiency, gain, and sidelobe level especially at low elevation angle [11], poor coverage and capacity performance is experienced at the edge of coverage. Secondly, with the effect of beam broadening, edge cells are several times bigger than cells closer to the sub-platform point (SPP), which is at the nadir of the HAP. This results in uneven cell loading, with potentially more users sharing the limited spectrum resources in edge cells compared to cells closer to the SPP despite the reducing signal strength, with increasing distance from the SPP. These affect the system performance and make guaranteeing a minimum quality of service (QoS) within the extended area challenging. Thus, a cellular architecture that mitigates these effects and enhances the QoS is required.

This paper investigates some tier-based schemes and approaches to improve coverage and capacity by mitigating the effects of ICI and uneven cell loading due to the disproportionality of the cell sizes across the coverage area. As a continuation of the work in [10], we propose a two-tier HAP cellular architecture, which forms two tiers of cells over an extended area with users associating with the best cell and tier. While tiered architectures have been studied in the past, those typically focus mainly on cell overlay and underlay [12]. Unlike in traditional tier-based architectures, a tier here is defined as a collection of many cells forming a contiguous cellular structure as in [10], which provides coverage and capacity over the entire HAP extended service area. The proposed two tiers are characteristically homogeneous in terms of transmit power per cell, coverage, etc., and are both formed from the same service link antenna infrastructure hosted in the HAP. These introduce unique difficulties in resource and interference management as well as feeder link dimensioning for practical deployment. The proposed architecture enhances edge-of-cell connectivity, uneven cell loading, and coverage holes by considerably enhancing CINR for some user. It significantly outperforms the typical one-tier architecture presented in [10]. Specifically, the contributions of this paper are:

- We propose a two-tier HAP cellular architecture formed using a single antenna array infrastructure, which gives users the flexibility of connecting to the best cell and tier. The architecture comprising two independent tiers of contiguous cells significantly improves coverage by enhancing edge user signal quality to achieve ubiquitous coverage, mitigates against uneven cell loading, enhances cell edge connectivity and the total system capacity.

- We develop an algorithm that implements the two-tier architecture and propose a low complexity user-association where UEs exploit the co-location benefits of a quasi-stationary HAP to attach to a cell and tier that maximises both coverage and capacity.

- We investigate different resource and interference management schemes, showing how full spectrum reuse, spectrum partitioning, and inter-cell interference coordination (ICIC) perform with one-tier and the proposed two-tier architectures.

The rest of the paper is organised as follows. Section 2 presents some related work in the literature. Section 3 provides a background to the tier-based HAP cellular architecture, with an overview of the proposed two-tier architecture and an intuitive discussion about its practicality. The system model of the two-tier architecture is presented in section 4. Section 5 presents the performance of the proposed architecture, highlighting its benefits over a one-tier architecture. The paper is concluded in section 6.

2 RELATED WORK

The deployment of multiple HAP beams for cellular communication, which has been investigated by some prior studies [1], [13], [14], [15], is fundamental for enhanced coverage and capacity. The pioneering work in [1] proposed the use of scanning beams to regularly visit an arrangement of cells on the ground and activate each visited cells. With many cells potentially over a wide area in a tiered architecture, system complexity increases as scan time per cell reduces, thereby, requiring user devices to buffer traffic while waiting for the next cell activation. Studies in [13] proposed an algorithm that creates a layout of cells in a single tier to minimise coverage gaps. The layout is based on a uniform hexagonal grid over a very limited area of less than 15 km radius. Some other strategies of forming cells across the HAP coverage area such as deploying beams randomly, in a regular pattern, or over optimised k-means clusters of users were investigated in [14]. While the resulting cellular foot-

print provided coverage over an area of about 30 km radius, there were considerable coverage gaps introduced to ensure HAP coexistence with terrestrial systems. Similarly, considering a 30 km radius area, a beamforming technique that uses particle swarm optimisation to find the optimum weights for antenna elements in an array was proposed in [15]. Clearly, these studies are unsuitable for an extended coverage area of over 30 km radius due to their inconsideration of beam broadening and the resulting challenges. Therefore, in [10], we proposed a beam-pointing algorithm that qaudriples the area of coverage with over 60 km radius. To solve the resulting poor cell edge performance and uneven loading of such extended coverage, a tier-based HAP cellular architecture is proposed in this paper.

Generally, tiered networks can improve spectral efficiency, coverage and capacity, minimise handover and ensure service continuity subject to effective interference and resource management [16]. A two-tier cellular architecture comprising a HAP cell overlaying multiple low altitude platform (LAP) cells was proposed in [12]. The study developed algorithms to manage inter-tier interference (ITI) based on transmit power optimisation for spectrum overlay and underlay access techniques. The feasibility and challenges of such architecture including the platform size, weight and power (SWaP) constraints were highlighted in [17], [18]. Extended multi-tier architectures with a larger HAP cell overlaying both LAP and terrestrial cells were presented in [19], [20]. While [19] also proposed dynamic cell placement and sizing algorithms for load balancing and better QoS as well as frameworks for coverage and capacity analysis, [20] highlights the potential of tiered architecture in 5G and beyond. The use of machine learning to solve the problem of user association typically between a number of low-power small cells within a larger high-power macro cell was proposed in [21], [22]. Studies in [23] discussed the exploitation of ICIC techniques such as fractional frequency reuse to manage interference between the macro and small cells. Interestingly, these studies are all based on similar architectures where a larger cell completely overlays smaller cells with each tier delivered from different infrastructures, which has significant cost implications. Conversely, this paper presents a two-tier architecture formed using many independently steerable beams from the same antenna array infrastructure with the two tiers equally comprising many disproportionately sized cells tessellated over an extended service area. In practice, this will require a massive phased an-

tenna array that can be supported by a HAP, given its SWaP constraints, such as the state-of-the-art 2048 dual-polarised element array in [24].

3 TIER-BASED HAP SYSTEM BACKGROUND

3.1 Overview

A fundamental challenge with the typical one-tier HAP cellular architecture for extended coverage and capacity proposed in [10] is the poor cell edge performance and uneven cell loading, which worsens with increasing distance away from the SPP. Consequently, a two-tier architecture is proposed where edge users in one tier potentially become centre users in the other tier. It is comprised of alternative contiguous structures of cells of similar coverage, radio and antenna beam characteristics. Users have the flexibility of associating with a tier based on given conditions such as satisfying a minimum QoS or cell loading requirement. The availability of alternative cells and tiers with orthogonal channel conditions that users can be associated with enhances their robustness and cell edge connectivity by significantly enhancing received signal quality, thereby mitigating coverage holes.

Fig. 1a illustrates the proposed architecture using two tiers of three contiguous cells with similar antenna beam characteristics. A one-tier architecture would typically be made up of only the footprint of one of the tiers, however, significantly better overall performance can be achieved by using the proposed two-tier architecture. Fig. 1b further highlights the potential benefits of the proposed architecture in terms of the robustness and flexibility of the system. Imagine the second tier as an offset in angle of the first tier, if the beam boresight (i.e. axis of maximum radiated power and gain) of the beamforming antenna is at the centre of the cells, the gain at the edge of the cells is expectedly less than at the boresight depending on the size of the beam and the number of the beamforming antenna elements. Hence, it is expected that the signal quality of users at the edge of a cell is significantly less compared with those at the centre. Therefore, the proposed two-tier architecture seeks to jointly enhance the CNR and CINR of some users by providing alternative options for edge users to enhance their received signal quality, as depicted by user equipment (UE) 1 and 2 in Fig. 1b moving from the edge of cells in Tier 1 (T1) to the centre of a cell in Tier 2 (T2). Some users such as UE 3, which ordinarily would have no coverage in a single tier network based on T1, are provided coverage by T2. In summary, the

(a) Example footprint of the tiered architecture.

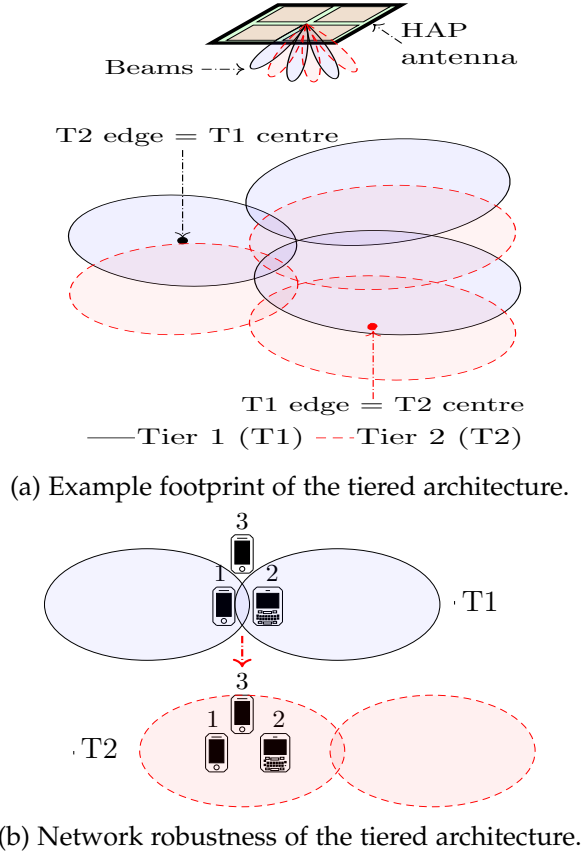

(b) Network robustness of the tiered architecture.

Fig. 1: The tier-based HAP cellular architecture. (a) highlights the architecture using two tiers of three contiguous cells. (b) shows the robustness, and flexibility of the architecture where users can associate with any cell and tier that maximises experience.

two-tier architecture improves CINR by exploiting the antenna beam pointing more effectively without increasing transmit power.

3.2 Delivering a Tier-based Architecture

This section presents an intuitive discussion and practical considerations on how a tier-based HAP architecture can be delivered by exploiting multiple simultaneous beams from an array antenna aperture and the effect of platform instability.

Irrespective of how multiple beams are delivered, proper isolation between beams and tiers is needed for orthogonality to minimise interference. This is achieved by ensuring a low beam crossover level in the multi-beam antennas (MBA). Passive MBA requires multiple beamforming networks (BFN) such as Butler or Blass matrices to deliver the beams required for HAP coverage over an extended service area. This results in a complicated antenna system layout with increased insertion loss, which can be mitigated by increasing

the aperture but within the HAP constraints. Two separate apertures can be used to form the two-tier architecture, with each delivering the beams needed for one tier, and beams from both apertures could further be isolated with different polarizations [25]. Such solution will result in an antenna system with reduced complexity, beam crossover level, and low power budget inherent in BFN. The demerit is the resultant large form factor and lack of flexibility of BFNs as the number of beams and their pointing direction must be predefined prior to manufacture [26]. On the other hand, multi-beam phased antenna array (MBPAA) and digital MBA (DMBA) are more flexible as they are electronically scanned and have smaller form factor, but they are more complicated with higher power requirement compared with PMBA. In both MBPAA and DMBA, for the two-tier architecture, the number of beams and their directions could be provided as inputs. Delivering the two-tier architecture is practicable with some of these antennas, however, given the limitations of HAPs, SWaP constraints must be considered among other factors such as platform instability [18].

The HAP antenna array orientation and attitude can be affected by the platform's instability or displacement due to pitch, roll or yaw. This can offset the cellular footprints from the antenna beams resulting in the change of the coverage of individual cells, multiple forced handovers, and poor performance [27]. However, these can be mitigated by controlling the platform thrusting [28] or actively compensating for the HAP displacement with the antenna to keep the beams fixed on the ground irrespective of the platform motion [24], [29].

4 TWO-TIER HAP ARCHITECTURE MODEL

This section presents the proposed two-tier architecture system model and describes the techniques for beam deployment, tier formation, user association, resource allocation, and performance evaluation.

4.1 System Model and Performance Metrics

4.1.1 Beam Deployment

Consider a quasi-stationary HAP at an altitude h_p and at the centre of a service area of radius R. The HAP flying horizontally supports a uniform planar phased antenna array of $M \times N$ elements with the array facing downward and parallel to the ground surface. Multiple beams are formed from the array and pointed such that the footprints of the resulting cells provide coverage to a set of users $\mathcal{I}$ within
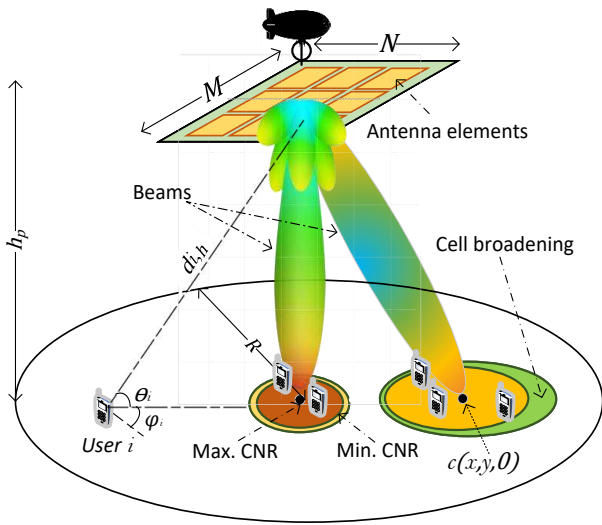
Fig. 2: HAP antenna array beamforming for cellular coverage.

the service area as shown in Fig. 2. These beams are pointed at a set of coordinates $\mathcal{C}$, which are generated such that the resulting footprints of the beams produce a regular tessellated structure of contiguous cells $c \in \mathcal{C}$ over an extended area. Each user associates with a cell that maximises its signal quality. The HAP transmit antenna gain profile G_i for signal quality evaluation, as observed by user $i \in \mathcal{I}$, is given by [30] as follows,

$$G_i = g_e \mathrm{AF}_{x,i} \mathrm{AF}_{y,i}, \tag{1}$$

where $\mathrm{AF}_{x,i}$ and $\mathrm{AF}_{y,i}$ are expressed respectively as

$$\mathrm{AF}_{x,i} = \sum_{n=1}^{N} I_n e^{j(n-1)(kd_x \sin \theta_i \cos \varphi_i + \beta_{x,i})}, \tag{2}$$

$$\mathrm{AF}_{y,i} = \sum_{m=1}^{M} I_m e^{j(m-1)(kd_y \sin \theta_i \sin \varphi_i + \beta_{y,i})}, \tag{3}$$

where the angular wave number $k = 2\pi/\lambda$, λ is the wavelength, d_x and d_y are the inter-element spacings in the x- and y- axes of the antenna array with array factors $\mathrm{AF}_{x,i}$ and $\mathrm{AF}_{y,i}$ respectively at user i. I_n and I_m represent the excitation amplitudes of the antenna elements, θ_i and φ_i define elevation and azimuth angles evaluated with the user coordinates. $\beta_x = -kd_x \sin(\theta_i^0) \cos(\varphi_i^0)$ and $\beta_y = -kd_y \sin(\theta_i^0) \sin(\varphi_i^0)$ are phase shifts with θ_i^0 and φ_i^0 being the boresight elevation and azimuth angles respectively. Isotropic antenna elements with the gain of a single element $g_e = 1$ are assumed.

The coordinates of multiple beam boresight points on the ground are obtained as a set of cell coordinates $\mathcal{C}$ from the proposed algorithm in [10] and converted into their corresponding elevation and azimuth angles relative to the HAP. These are supplied to the beamformer with (1) to obtain the distribution of HAP antenna transmit gain on the ground. The beams formed are then used to create HAP cells. To define a cell, let $\tilde{\mathcal{A}}_b$ be the footprint of beam b on the ground, p be any interior point in $\tilde{\mathcal{A}}_b$ and Γ_p be the CNR at point p. The cell c is a bounded region around the beam boresight with boundary $\partial c := p \in \tilde{\mathcal{A}}_b : \forall p, \Gamma_p \geqslant 9$ dB. The 9 dB CNR threshold is based on specification 3GPP TS 05.05 [31], which specifies a minimum mobile station receiver reference sensitivity of -102 dBm that ensures a bit error rate of $\leqslant 10^{-4}$ [32]. Γ_i for user i is evaluated as

$$\Gamma_i = \frac{P_i G_i \mathcal{G}_i}{\mathcal{N}_i L_{i,h}}, \tag{4}$$

where P_i is the HAP transmit power, $\mathcal{G}_i$ and $\mathcal{N}_i$ are the user receive antenna gain and noise power respectively. Considering the high HAP line-of-sight (LoS) probability even at low elevation angles in rural and sub-urban areas [33], the channel between user i and the HAP h is modelled as a large scale fading channel with loss $L_{i,h}$ dominated by free-space path loss and log-normally distributed fading due to shadowing [34]. This follows the non-terrestrial network (NTN) channel model reported in 3GPP TR 38.811 [35], which allows for a realistic large-scale representation of the HAP propagation channel. Small-scale fading is not considered in this dominant LoS scenario since the focus is on cellular structure in general and the long term mutual interference effects of the cells on each other. Furthermore, considering the fixed users and a quasi-stationary HAP, small-scale fading occurs but with limited impact as validated by results from a practical HAP flight trial reported in [36]. With both user and platform mobility, a different channel model such as in [37] becomes more appropriate but beyond the scope of this work. $L_{i,h}$ is expressed as

$$L_{i,h} = \left(\frac{4\pi d_{i,h} f}{v}\right)^2 X_\sigma, \tag{5}$$

where $d_{i,h}$ is the slant distance between user i and the HAP h in km, f is the carrier frequency in GHz, v is the speed of light in m/s and X_σ is a log-normally distributed random variable with 0 dB mean and standard deviation σ_x of 4 dB, representing fading due to shadowing [38].

4.1.2 User Distribution

Considering a user density of λ users/km^2, a set of users with 2D coordinates $\mathcal{I}$ are randomly distributed over the HAP service area of A km^2. The number of users $|\mathcal{I}|$, where $|.|$ denotes cardinality, is independently and identically distributed over the space, denoting the HAP service area, according to a Poisson distributed random variable with mean λA. This follows a bivariate Poisson point process (PPP) $\Phi_p \in \mathbb{R}^2$. The PPP model is used to illustrate the performance improvement, through the reduction of edge of cell effects and load balancing, by the schemes proposed in the paper. More complex user and HAP mobility models are possible for further performance evaluation but not covered here.

4.1.3 Performance Metrics

In order to evaluate the performance of the proposed two-tier architecture, some metrics are used in addition to CNR and CINR. While CNR for user i is defined in (4), CINR is defined as

$$\gamma_i = \frac{\mathcal{P}_i}{\sum\limits_{j=1}^{J} \mathcal{P}_{j,i} + \mathcal{N}_i}, \qquad (6)$$

where $\mathcal{P}_i$, which is the received power of user i from its associated cell, is expressed as

$$\mathcal{P}_i = \frac{P_i G_i \mathcal{G}_i}{L_{i,h}}, \qquad (7)$$

and $\mathcal{P}_{j,i}$ is the total interference power experienced at user i, which is summed over all active downlink transmissions in J other interfering cells with index $j=1,2,3\cdots,J|\mathcal{P}_{j,i} \neq \mathcal{P}_i$ [14].

Additionally, system throughput, user allocation probability, and Jain's fairness index are also used. Throughputs T_i are evaluated using the Truncated Shannon Bound equation [39] expressed as

$$T_i = \alpha b_i \begin{cases} 0, & \gamma_i < \gamma_{\min} \\ \log_2(1+\gamma_i), & \gamma_{\min} \leqslant \gamma_i \leqslant \gamma_{\max}, \\ \log_2(1+\gamma_{\max}), & \gamma_i > \gamma_{\max}, \end{cases} \qquad (8)$$

where $\alpha=0.65$ is the implementation loss, b_i is the bandwidth allocated to user i, $\gamma_{\min}=1.8$ dB is the minimum allowed CINR for resource block (RB) allocation and $\gamma_{\max}=22$ dB is the CINR resulting in the maximum achievable throughput, γ_i is user i's CINR [39]. The total system throughput is evaluated as the sum of the overall throughputs of all users.

The user allocation probability $\frac{i_{RB}}{|\mathcal{I}|}$ is the ratio of the number of users allocated at least one RB i_{RB}

to the total number of users in the system $|\mathcal{I}|$. Jain's throughput fairness index J_n is given in [40] as

$$J_n(\tilde{T}_1, \tilde{T}_2, \cdots, \tilde{T}_I) = \frac{\left(\sum\limits_{i=1}^{I} \tilde{T}_i\right)^2}{I \sum\limits_{i=1}^{I} \tilde{T}_i^{\,2}}, \qquad (9)$$

where $\tilde{T}_i$ is the mean throughput of user i. J_n is maximised if all users have equal throughput.

4.2 Tier Formation

The formation of the proposed two-tier HAP cellular architecture for the extended coverage shown in Fig. 3 requires the contiguous cell centre coordinates obtained from running the cell-pointing algorithm we originally proposed in [10]. The algorithm generates a set of coordinates used by the HAP antenna system for beam-pointing, to create a single tier of contiguous HAP cell structure across an extended service area.

In order to then form the two-tier cellular architecture, the set of coordinates used in forming the single-tier architecture for tier 1 (T1) is rotated by an offset angle ξ to obtain another set of coordinates for beam-pointing that creates a different contiguous HAP cell structure for tier 2 (T2) using

$$c' = \begin{bmatrix} \cos\xi & \sin\xi \\ -\sin\xi & \cos\xi \end{bmatrix} c, \qquad (10)$$

where $c' \subseteq \mathcal{C}^2$ and $c \subseteq \mathcal{C}^1$ are column vectors denoting the rotated x- and y- axes coordinates for beamforming to form T1 and T2 respectively. The offset angle ξ can be defined based on network requirements. The objective here is to improve coverage and capacity by heuristically enhancing both user CNR and CINR, in addition to loading balancing between the tiers. The resulting two sets of coordinates, each forming one tier, are used for cell formation. In Fig. 3, notice that the cells in one tier result from the rotation of the other tier's cells such that the edges of cells in one tier corresponds to the centre of a similar cells in the other tier. This is achieved by setting $\xi=\rho$ for fair coverage and capacity enhancements, where ρ is the angle subtended at the HAP by the centre and edge of the broadside cell, which is equal for all cells. However, depending on the required QoS, or coverage pattern for instance, a different offset angle may be more appropriate. The detailed tier formation algorithm is presented in Algorithm 1 with complexity analysis in Section 4.2.1. The two-tier cell centre coordinates obtained from
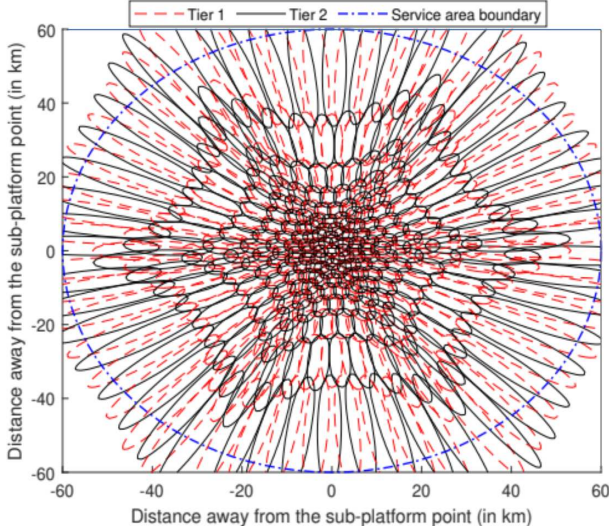
Fig. 3: The two-tier architecture cellular footprint.

Algorithm 1 are used by the antenna systems, which forms and points beams at these coordinates to produce the cellular architecture shown in Fig. 3.

Algorithm 1 Tier Formation Algorithm

1: Run the cell-pointing algorithm in appendix to obtain a set of tier 1 (T1) cell coordinates $\mathcal{C}^1$.
2: Obtain the broadside cell subtended angle ρ.
3: Set ofset angle $\xi = \rho$: Valid range is $\xi | 0° < \xi < 2\rho$.
4: Initialise the set of new cell coordinates $\mathcal{C}^2 = \emptyset$ for tier 2 (T2).
5: **for** each $c \subseteq \mathcal{C}^1 | c \in \mathbb{R}^2, c \neq \emptyset$ **do**
6:     Evaluate $c_n := c$ rotated by angle ξ using (10).
7:     Update $\mathcal{C}^2 := \mathcal{C}^2 \cup c_n$.
8: **end for**
9: Obtain set of all cell coordinates $\mathcal{T}^{1,2} := \mathcal{C}^1 \cup \mathcal{C}^2$.
10: Collect $\mathcal{T}^{1,2}$, $\mathcal{C}^1$, $\mathcal{C}^2$: Coordinates used by the antenna for beam pointing to form T1 and T2.

4.2.1 Complexity of Tier Formation Algorithm

Interestingly, Algorithm 1, which can be run offline with the obtained beam boresight point coordinates stored in a look-up table, has the same asymptotic time complexity as the cell-pointing algorithm proposed in [10] and reproduced in the appendix. The complexity is $\mathcal{O}(c)$, where c denotes the numbers of cells within the service area. Thus, the greater the number of cells or the wider the service area, the higher the complexity.

4.3 User Association

Each user in the network associates with a cell and a corresponding tier that maximises its CNR

and CINR respectively. Typically, user i's Γ_i and γ_i, evaluated using (4) and (6), greedily determine which cell and tier respectively the user associates with. User i associates with a cell $\iff \Gamma_i \geqslant \Gamma_{\text{thr}}$, where Γ_{thr} is the minimum CNR threshold required for user-cell association. In the association process, user i's Γ_i in all the covering cells in both tiers are initially obtained. User i then temporarily associates with the two cells, one in each tier, providing the highest Γ_i. Then, the user's γ_i in both cells are evaluated with the user permanently associating with the tier and and its corresponding cell providing the highest γ_i. If user i is located within a region where two or more cells in the same tier overlap, it associates with the cell that maximises its received power P_i^r. Invariably, users in an overlap region can detect all of the overlapping cells. Algorithm 2, which is implementable in a HAP central controller, either in a regenerative or bent-pipe architecure, performs the user association. The controller can then forward association messages containing the cell and tier information to users for connecting to the network. The complexity of Algorithm 2 is analysed in Section 4.3.1.

Algorithm 2 User Association Algorithm

1: Declare $\mathcal{T}^{1,2}$, $\mathcal{I}$, T: Tier information, associating user information, and number of tiers.
2: Set Γ_{thr}: Minimum CNR threshold.
3: Initialise the association information matrix $B_{i,t,c}$.
4: **for** each user $i \in \mathcal{I}$ **do**
5:     **for** each tier $t \in T$ **do**
6:         **for** each cell $c \in \mathcal{C}^t | \mathcal{C}^t \subseteq \mathcal{T}^{1,2}$ **do**
7:             Compute Γ_i using (4).
8:             **if** $\Gamma_i \geqslant \Gamma_{\text{thr}}$ **then**
9:                 Record Γ_i and the corresponding cell c, i.e. $A_i(c) := \Gamma_i$.
10:             **end if**
11:         **end for**
12:         Obtain the cell c_i that maximises Γ_i from Line 9, i.e. $c_i = \arg \max_c A_i(c)$.
13:         Compute the γ_i in cell c_i using (6).
14:         Record the user's c_i and γ_i in tier t, i.e. $S_i(t) = [c_i, \gamma_i]$.
15:     **end for**
16:     Obtain the tier t and the corresponding cell c_i that maximises the user's γ_i from $S_i(t)$.
17:     Update $B_{i,t,c}$ with user i's t, c_i, and γ_i.
18: **end for**
19: Collect $B_{i,t,c}$: User association information matrix used for user association.

4.3.1 Complexity of User Association Algorithm

The complexity of Algorithm 2 is $\mathcal{O}(itc)$, where i, t, c are the total number of users, tiers and cells respectively. To reduce the complexity of Algorithm 2 in practical HAP deployments, instead of evaluating the perceived Γ_i from all the cells for user i, the evaluation will be carried out for only the $|\mathcal{C}|$ cells providing signals with the highest quality for the UE based on an appropriate metric such as reference signal received power (RSRP). Consequently, Line 6 can be for each $c \in \mathcal{C} | \mathcal{C} \subseteq \mathcal{C}^t$, where $|\mathcal{C}|$ is controlled by setting the minimum RSRP threshold based on network operator's requirement or standard for the specific technology such as long-term evolution (LTE), 5G, or 6G. For instance, LTE requires RSRP >-140 dBm [41], which limits $|\mathcal{C}|$ to just a few cells. Therefore, the reduced complexity becomes $\mathcal{O}(itc_s)$, where $c_s \ll c$ is the number of cells in the subset of the total number of cells in the service area covering user i. In practical implementation, this algorithm will run online to carry out user association as users enter and leave the network.

4.4 Resource Allocation

In a HAP system based on the proposed two-tier architecture, three key resource allocation decisions must be made, starting with the decision on how the system resources are shared between the tiers and then the cells. In LTE and beyond systems, implementing the proposed architecture would involve the sharing of RBs between the tiers. Subsequently, each tier then decides how to allocate resources between its cells, and eventually each cell in a tier assigns its allocated resources to users accordingly.

Full spectrum reuse (FR) and partial spectrum reuse (PR) schemes are considered for the sharing of RBs at each level of abstraction in the two-tier architecture. The FR scheme allows each cell in each tier to fully reuse all available RBs with a cell allocating RBs to its associated users based only on the local RB usage in the cell. Conversely, the system RBs in the PR scheme are partitioned between the two tiers, with each cell fully reusing only its tier's allocated RBs. Defining mathematically, let $R_b = \{1, 2, 3, \cdots, N_{R_b}\}$ denote the whole set of system RBs, where N_{R_b} is the maximum number of RBs available. In the FR scheme, each cell in each tier t is assigned a set $\tilde{R}_b^t = R_b$. In the PR scheme, $\tilde{R}_b^1$ and $\tilde{R}_b^2$ are the sets of RBs assigned to each cell in tiers 1 and 2 respectively such that $\tilde{R}_b^1 \cup \tilde{R}_b^2 = R_b$ and $\tilde{R}_b^1 \cap \tilde{R}_b^2 = \emptyset$. The system RBs are shared between the tiers such that each tier is assigned $\lfloor \frac{i_t}{I} N_{R_b} \rceil$ RBs,

where i_t is the number of users associated with the tier, I is total number of users in the network, and $\lfloor . \rceil$ represents rounding to the nearest integer.

Irrespective of the allocation scheme, the HAP system expectedly will suffer from intra-tier ICI. Additionally, the FR scheme also suffers from considerable inter-tier interference (ITI) due to the significant overlap of the main lobes of the beams that form the two tiers. Therefore, the ITI, which significantly degrades the system performance, should be mitigated to enhance performance [42] and fully exploit the benefits of the two-tier architecture. The PR scheme eliminates ITI by ensuring orthogonality between the tiers, however, it still suffers from intra-tier ICI. An appropriate scheme should mitigate both ICI and ITI to enhance system performance. Here, the possibility of using ICIC [43] for interference mitigation in the HAP two-tier network is investigated. For ICIC, irrespective of the reuse scheme, a cell is partitioned into centre and edge regions based on a region partitioning CINR threshold $\gamma_{\text{thr}}^{\text{rp}}$, which can be varied as appropriate. A user i is classed as being in the edge region and thus an edge user if $\gamma_i \leqslant \gamma_{\text{thr}}^{\text{rp}}$, otherwise, it is in the centre region and classed as a centre user. Considering the steep power roll-off from the centre to edge of a HAP cell, neighbouring cells can reuse RBs only in the centre regions without coordination while coordination is required for allocations in the edge regions. The coordination required can be implemented in the network controller at the HAP with a global view of all the cells. There is a possibility of greater gains being achievable by using further enhanced ICIC (FeICIC) introduced in the 3GPP Release 11, which includes interference cancellation.

5 PERFORMANCE EVALUATION

To evaluate the performance of the two-tier architecture with different reuse schemes and ICIC, considering only downlink scenario, we set up a snapshot-based simulation with the default parameters given in Table 1. The chosen radio parameters are within standard ranges as per 3GPP specifications like TS 05.05 and TR 38.811. Each result presented is evaluated from the cumulative outcomes of 50 independent snapshots, which keeps errors to statistically within only 1% of the average values.

Following cell and tier creation, each cell accommodates a maximum of 25 simultaneously active users and frequency spectrum resources are shared between users in a cell at RB level. Users requesting resources are assumed to be scheduled by the

TABLE 1: Key simulation parameters.

Key parameters	Simulation Values
HAP height h_p	20 km
HAP transmit power P_i	33 dBm
Receive antenna gain $\mathcal{G}_i$	1.5 dBi
Cell association CNR threshold Γ_{thr}	9 dB
Noise floor	-95 dBm
Frequency f	2.1 GHz
User density λ	2 users/km^2
Tier offset angle ξ	3.5°
System bandwidth	20 MHz
Maximum active users per cell	25
Number of resource blocks	100
Number of antenna elements $M \times N$	1600

(a) One-tier architecture.

(b) Two-tier architecture.

Fig. 4: Surface plots of user CINR γ_i with one-tier (a) and two-tier with partial reuse (b) architectures.

centralised network controller, which is located at the HAP, parsing through requests and scheduling one user at a time. The best available RB, based on CINR, is then allocated to each associated user by its home cell. The schedule is parsed multiple times by the controller to enable home cells to allocate extra RBs if available to active users, but with priority on the users not allocated a RB in the previous parse. For user i to be allocated an RB, it must satisfy the minimum $\gamma_i \geqslant 1.8$ dB requirement [39], otherwise, the user is blocked.
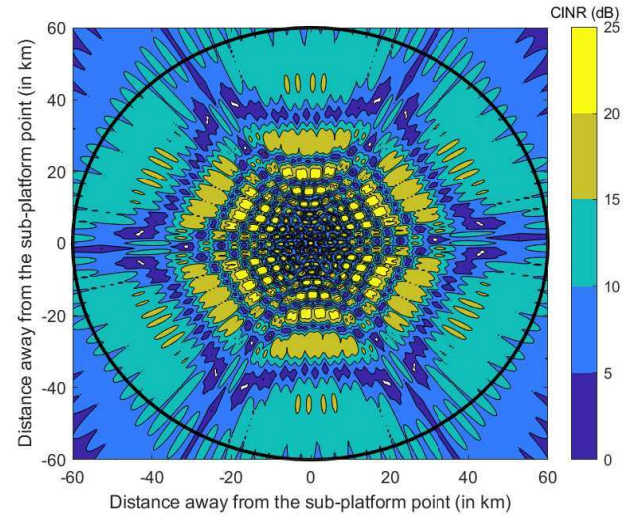
5.1 System Performance

5.1.1 Comparing one-tier and two-tier architecture

In this subsection, the coverage, throughput, and fairness performances of the one-tier and two-tier architectures are presented. Following user associations and RB allocations, γ_i and T_i are evaluated for each user using (6) and (8) respectively.

1) *Coverage and CINR Distribution*. Fig. 4 shows the surface plots of γ_i in the one-tier and proposed two-tier PR architectures. Cells in the one-tier architecture fully reuse the available spectrum while the spectrum is partitioned for orthogonality between tiers in the two-tier architecture, with cells fully reusing the spectrum allocated to their associated tier. Both architectures have the same coverage area as indicated by the solid line circle. In the two-tier architecture, γ_i is evaluated for partial reuse without considering ITI due to the orthogonality of the tiers. Fig. 4a shows that considerable areas within the one-tier HAP extended service area have poor signal quality with the existence of significant coverage holes resulting from the effects of ICI and signal quality degradation especially at cell edges. On the other hand, the two-tier architecture provides near-ubiquitous coverage with enhanced edge-of-cell connectivity as shown in Fig. 4b and confirmed in Fig. 5, which shows the proportion of edge users to the total number of users in the one-tier and two-tier architectures for different region partitioning thresholds. Notice in Fig. 4b that with two tiers, sufficient signal quality is received even at extended distances from the SPP, and identifying the edges of cells is not as straightforward as in the one-tier scenario. Clearly, the received signal quality increases, resulting in minimised cell edge connectivity and improved fairness.

2) *Achievable User Throughput*. The achievable user throughput of the one-tier and proposed two-
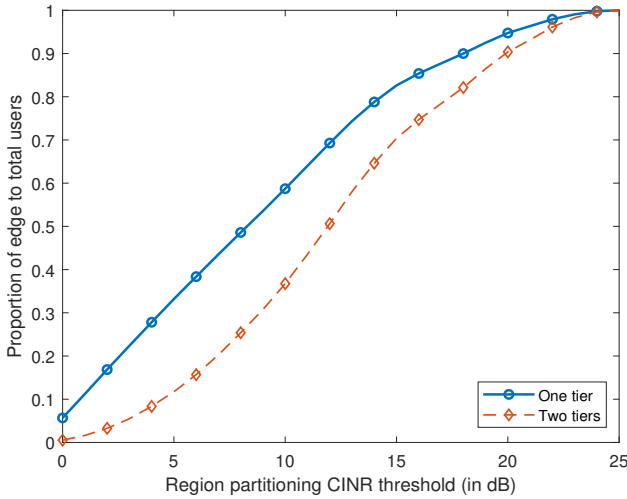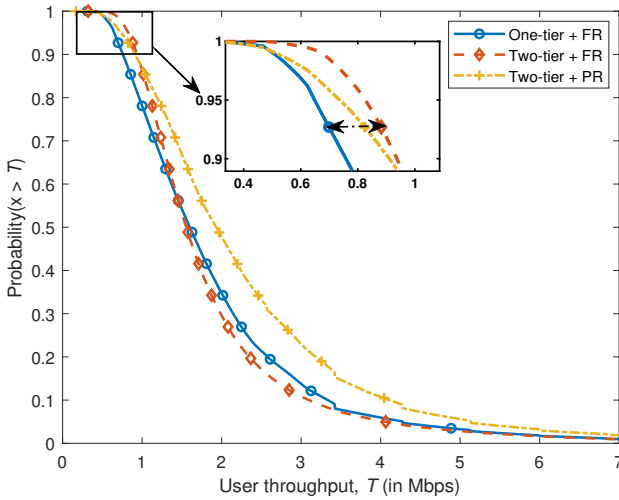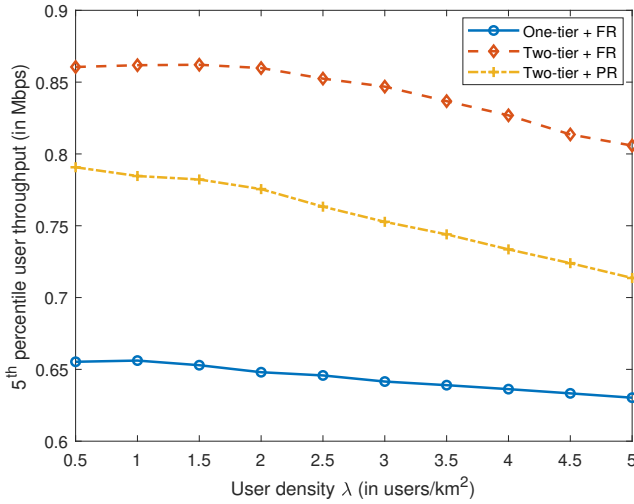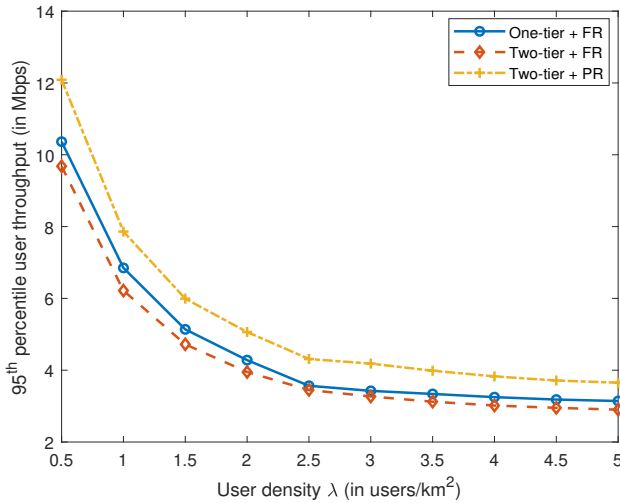
Fig. 5: Proportion of edge to total users.

Fig. 6: Complementary CDF of user throughput.

tier architectures with the FR and PR allocation schemes is shown in Fig. 6. For the bottom 10% of the users within the zoomed-in segment, which is mainly made up of users further away from the centre of cells, the two-tier FR experiences up to 27% higher user throughput compared with the other schemes for the same probability. The percentage improvement, calculated using the points between the bidirectional arrow in the inset, is as a result of both the higher multiplexing gain resulting from each cell's ability to choose and allocate a RB for a user from twice the full set of system RBs, in addition to the received signal strength improvements with the two-tier architecture. Unfortunately, this comes at the expense of most of the users suffering from considerable ITI, which degrades their signal

quality resulting in throughput reduction. On the other hand, the two-tier PR completely outperforms the one-tier FR scheme and performs significantly better than the two-tier FR scheme for the most part. Beyond the slightly poorer performance of the two-tier PR for the bottom 10% of the users within the inset, which is as a result of lower multiplexing, it notably outperforms the two-tier FR for the remaining 90% of the users many of which were edge users in the one-tier scenario.

Fig. 7(a) and 7(b) show the 5th and 95th percentile user throughput with varying user densities across the extended service area. In Fig. 7a, the two-tier FR provides over 30% higher throughput at given user densities compared with one-tier FR for the 5th percentile users that are closer to the edge-of-cell, due to the higher multiplexing gain and improved received signal strength. For the edge users, ICI minimises the number of usable RBs, therefore, having a bigger set of RBs gives these users more options and higher multiplexing gain, which results in better performance. For the 95th percentile users that are closer to the centres of the cells, two-tier PR offers up to 25% higher throughput compared with two-tier FR and one-tier FR as shown in Fig. 7(b). In the two-tier architecture, users at the centre of cells are minimally affected by ICI due to the steep roll-off of the HAP antenna radiation pattern, however, the resulting ITI degrades their throughput. The two-tier PR performs better because it orthogonally splits the available RBs between the two tiers, thereby effectively eliminating ITI. As shown in Fig. 7(b), one-tier FR slightly outperforms two-tier FR by about 7% again due to the considerable ITI. However, this should be offset against the over 30% improvement of the 5th percentile user throughput as shown in Fig. 7(a). In both figures, user throughput drops with increasing user density, which happens as more users share the available RBs leading to a drop in throughput.

3) *Achievable User Throughput*. Fig. 8 shows Jain's user throughput fairness index for varying user densities. At low user densities, with the number of RBs considerably greater than the users in a cell, the two-tier PR results in a higher throughput fairness index because users potentially have a sufficient number of RBs without ITI, due to the high probability of neighbouring cells allocating orthogonal RBs to their attached users. However, with increasing user density, the increased probability that RBs are shared less evenly between the two tiers results in a lower throughput fairness index compared with two-tier FR. This is worsened by the increasing

(a) 5th percentile user throughput.

(b) 95th percentile user throughput.

Fig. 7: The 5th and 95th percentile user throughputs.

Fig. 8: Fairness index of user throughputs.

5.1.2   The effect of ICIC

Having shown in Section 5.1.1 that the proposed two-tier architecture with either FR or PR scheme performs considerably better than a typical one-tier architecture, the effect of ICIC with the proposed architecture is therefore investigated in this section.

1) *Total System Throughput*. The total system throughput of the one-tier and two-tier architectures using FR, PR, and ICIC with varying $\gamma_{\text{thr}}^{\text{rp}}$ is shown in Fig. 9. At low $\gamma_{\text{thr}}^{\text{rp}}$, ICIC and FR have similar performance as the majority of the users are classified as centre region users, which implies that cells reuse the available RBs irrespective of the usages in other neighbouring cells of the other tier. For the two-tier FR with ICIC, the total throughput increases with increasing $\gamma_{\text{thr}}^{\text{rp}}$ as more edge region users emerge. Consequently, the number of users in the centre region where RBs can be reused are reduced. Thus, adjacent cells between the tiers avoid reusing RBs in the edge region with coordination. Similarly, for one-tier FR with ICIC, the total throughput increases with increasing $\gamma_{\text{thr}}^{\text{rp}}$ up to a point beyond which a further increase in $\gamma_{\text{thr}}^{\text{rp}}$ decreases the total throughput. This is the ideal centre-edge partitioning boundary. Clearly, the ideal boundary threshold for the one-tier architecture is smaller at about 10 dB than the 25 dB boundary for the two-tier architecture. This is because there are considerably more edge users in the one-tier architecture for the same threshold, which results in the one-tier architecture peaking earlier. Despite the improvement with ICIC compared with FR, the two-tier PR still outperforms all the other schemes due to the elimination of ITI, which degrades the

number of edge users having fewer options of RBs with low interference to choose from. The similarity in user throughput fairness between the two-tier PR and one-tier FR at high user densities is due to the trade-off between interference and available RBs. Users in the two-tier PR experience lower interference but also have limited options of RB availability, however, those in one-tier FR experience higher interference that is counterbalanced by the potential availability of full system RBs. On the other hand, with two-tier FR, all users have an opportunity of being allocated RBs from the whole available set in addition to their enhanced received signal quality due to interference minimisation by the two-tier architecture, which results in a fairer network in comparison with the other two schemes.
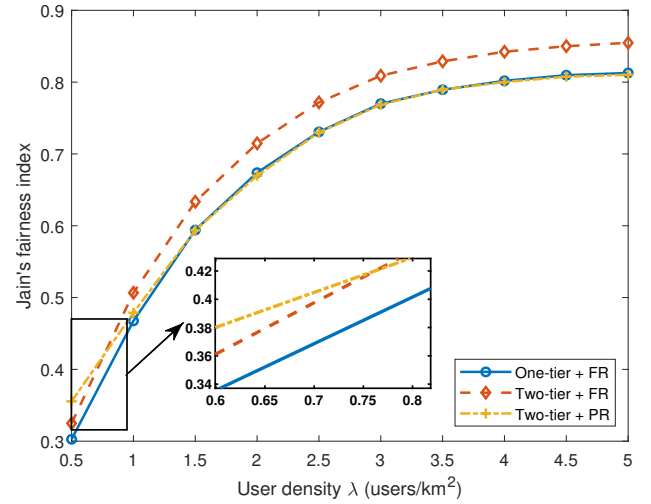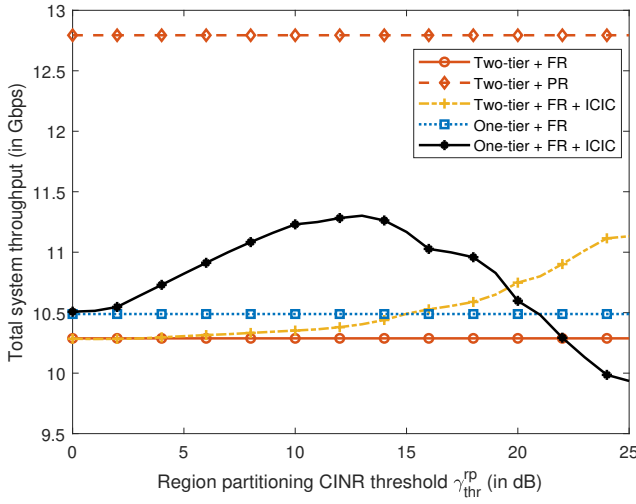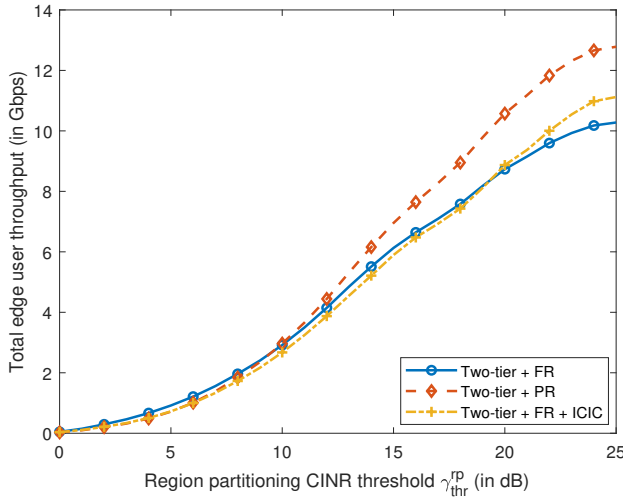
Fig. 9: Total system throughput.

(a) 10 dB region partitioning boundary.

Fig. 10: Total edge user throughput.

(b) 20 dB region partitioning boundary.

Fig. 11: The 5th percentile user throughputs with 10 dB and 20 dB region partitioning boundaries $\gamma_{\text{thr}}^{\text{rp}}$.
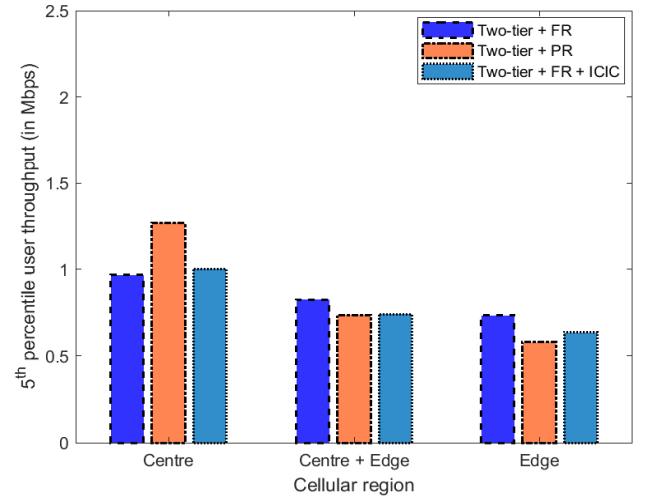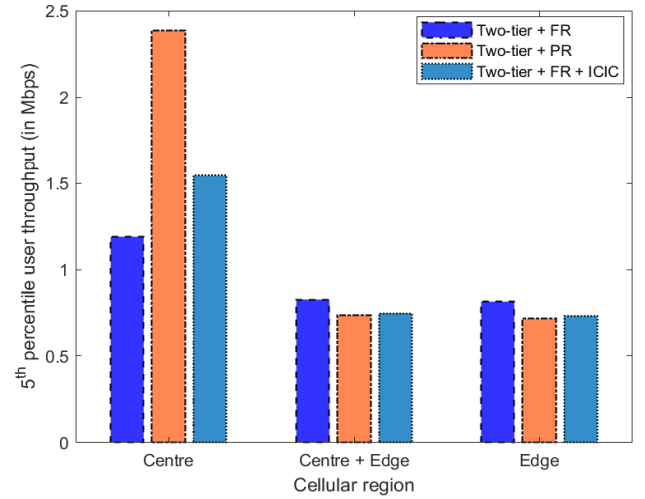
signal quality of users in the ICIC and FR schemes. The ITI is worsened by the contiguous nature of the architecture, which results in considerable overlap between cells. Since the total system throughput is dominated by the throughput of the centre users, the two-tier FR architecture is further affected by ITI and performs marginally poorer than the one-tier FR for this metric. Note that the constant throughput with FR and PR results ftom the fixed reuse pattern, which is unaffected by $\gamma_{\text{thr}}^{\text{rp}}$.

2) *Region-based Throughput.* Figs. 10, 11, and 12 show the effect of ICIC on the centre and edge user performance. Fig. 10 shows that the edge user throughput performance is similar for PR and ICIC with FR marginally better due to higher multiplexing gain, until the breakaway point of PR at about

$\gamma_{\text{thr}}^{\text{rp}}$=10 dB and ICIC at $\gamma_{\text{thr}}^{\text{rp}}$=20 dB. Considering the steep roll-off of power in a HAP cell, edge user performance increases with the elimination of as many interferers as possible. Since the ICIC scheme as implemented only avoids the highest interferer, edge users still experience significant interference from other cells both within and outside it's tier, which limits their performance. These edge region users at low $\gamma_{\text{thr}}^{\text{rp}}$ mainly benefit from having a wide range of RBs available as offered by FR. Moving towards the centre of cells with increasing $\gamma_{\text{thr}}^{\text{rp}}$, user performance is improved considerably by eliminating the highest interferer. Fig. 11 and 12 show that as $\gamma_{\text{thr}}^{\text{rp}}$ increases, the now fewer users in the centre region experience throughputs that are significantly
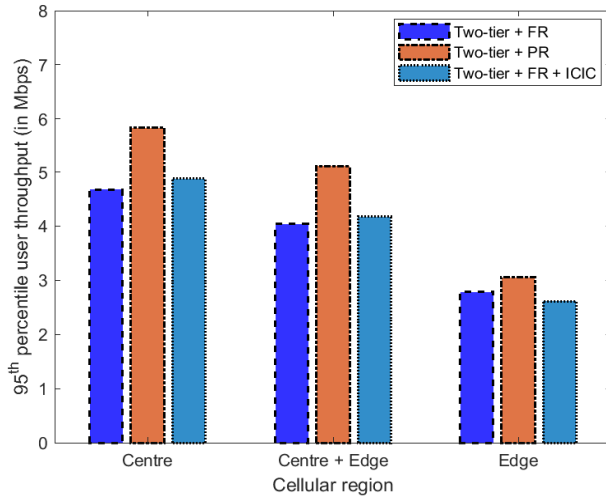
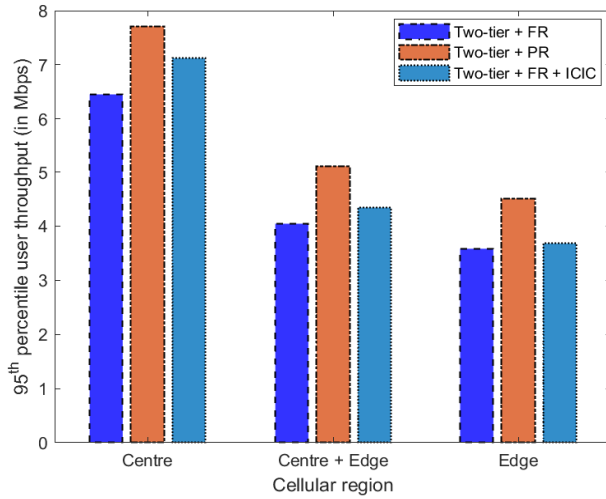(a) 10 dB region partitioning boundary.

(b) 20 dB region partitioning boundary.

Fig. 12: The 95$^{\text{th}}$ percentile user throughputs with 10 dB and 20 dB region partitioning boundaries $\gamma_{\text{thr}}^{\text{rp}}$.

higher than the edge region users because of the difference in their received signal quality and the minimal ICI. However, the combined throughput drops because more users are classed as edge users and forced to share RBs. Some of these users that could ordinarily reuse RBs even with ICI due to the steep-roll off of HAP received power are forced to share RBs with other poorer edge users. It is therefore important to appropriately set $\gamma_{\text{thr}}^{\text{rp}}$ to better dimension the centre and edge boundary to mitigate against the performance drop. Irrespective of the region, the two-tier PR results in superior 95$^{\text{th}}$ percentile user throughput as indicated in Fig. 12.

Although using ICIC with the proposed two-tier cellular architecture and FR performs better than just the two-tier FR as shown in Fig. 9–12, it is still limited by considerable inter-tier interference due to the overlap between cells of the two tiers.

6 CONCLUSION

This paper has proposed a new two-tier cellular architecture over a HAP extended service area. The architecture overcomes the edge-of-cell problems associated with conventional cellular architectures, which have up until now significantly limited the system capacity. It is made up of two tiers with similar cellular structures and characteristics but with an offset in angle between the centres of the cells in the two tiers. We proposed two algorithms with one implementing the two-tier architecture and the other performing user association and resource allocation. The resulting performance of the two-tier architecture with full spectrum reuse (FR) and schemes implementing spectrum partitioning resource allocation (PR) were compared with a typical one-tier architecture.

Simulation results show that the proposed HAP two-tier architecture significantly outperforms a typical one-tier architecture irrespective of the resource allocation scheme used. It also considerably mitigates the impact of ICI and beam broadening on the performance of the HAP extended coverage system. Considering the two-tier architecture, for the bottom 5–10% of users that are mostly at the edge-of-cells, the full reuse resource allocation scheme performs better than spectrum partitioning in terms of throughput due to the higher multiplexing gain. However, spectrum partitioning outperforms full reuse for the remaining 90–95% of users because of the orthogonality between the tiers, which eliminates inter-tier interference (ITI). On the other hand, both schemes suffer from inter-cell interference between the cells in a tier, however, whereas inter-cell interference coordination improves the performance of the full reuse scheme by about 10% with a region partitioning CINR threshold of 20 dB, it is still outperformed by spectrum partitioning by over 12% due to ITI. Thus, ITI is the main constraint of the proposed two-tier architecture. Further benefits of the proposed architecture include enhanced edge-of-cell connectivity and enhanced throughput fairness, which is evaluated using Jain's fairness index.

REFERENCES

[1] G. M. Djuknic, J. Freidenfelds, and Y. Okunev, "Establishing wireless communications services via high-altitude aeronautical platforms: a concept whose time has come?" *IEEE Commun. Mag.*, vol. 35, no. 9, pp. 128–135, Sep. 1997.

[2] L. Reynaud, S. Zaïmi, and Y. Gourhant, "Competitive assessments for HAP delivery of mobile services in emerging countries," in *IEEE ICIN*, Oct 2011, pp. 307–312.

[3] S. Chen et al., "Vision, requirements, and technology trend of 6G: How to tackle the challenges of system coverage, capacity, user data-rate and movement speed," *IEEE Wireless Commun.*, vol. 27, no. 2, pp. 218–228, 2020.

[4] L. Perlman and M. Wechsler, "Mobile coverage and its impact on digital financial services," https://ssrn.com/abstract=3370669, pp. 1–95, Apr. 2019, Accessed: 01-12-2020.

[5] B. El-Jabu and R. Steele, "Cellular communications using aerial platforms," *IEEE Trans. Veh. Technol.*, vol. 50, no. 3, pp. 686–700, May 2001.

[6] O. Anicho, P. B. Charlesworth, G. S. Baicher, and A. Nagar, "Antenna implementations for high altitude platform stations (HAPS) and considerations for future designs," in *IEEE iWAT*, 2022, pp. 246–248.

[7] J. Holis, D. Grace, and P. Pechac, "Effect of antenna power roll-off on the performance of 3G cellular systems from high altitude platforms," *IEEE Trans. Aerosp. Electron. Syst.*, vol. 46, no. 3, pp. 1468–1477, July 2010.

[8] J. Thornton, D. Grace, M. H. Capstick, and T. C. Tozer, "Optimizing an array of antennas for cellular coverage from a high altitude platform," *IEEE Trans. Wireless Commun.*, vol. 2, no. 3, pp. 484–492, May 2003.

[9] P. Rodriguez-Garcia et al., "Spurious beam suppression in dual-beam phased array transmission by impedance tuning," *IEEE Trans. Aerosp. Electron. Syst.*, pp. 1–15, 2022.

[10] S. C. Arum, D. Grace, P. D. Mitchell, and M. D. Zakaria, "Beam-pointing algorithm for contiguous high altitude platform cell formation for extended coverage," in *IEEE VTC*, Sep. 2019, pp. 1–5.

[11] Y. Wen, B. Wang, and X. Ding, "A wide-angle scanning and low sidelobe level microstrip phased array based on genetic algorithm optimization," *IEEE Trans. Antennas Propag.*, vol. 64, no. 2, pp. 805–810, 2016.

[12] H. Ahmadinejad and A. Falahati, "Forming a two-tier heterogeneous air-network via combination of high and low altitude platforms," *IEEE Trans. Veh. Technol.*, vol. 71, no. 2, pp. 1989–2001, 2022.

[13] M. Dessouky, M. Nofal, H. Sharshar, and Y. Albagory, "Optimization of beams directions for high altitude platforms cellular communications design," in *Proc. 23rd National Radio Sci. Conf.*, 2006, pp. 1–8.

[14] M. D. Zakaria, D. Grace, P. D. Mitchell, T. M. Shami, and N. Morozs, "Exploiting user-centric joint transmission-coordinated multipoint with a high altitude platform system architecture," *IEEE Access*, vol. 7, pp. 38 957–38 972, 2019.

[15] A. M. Ismaiel, E. Elsaidy, Y. Albagory, H. A. Atallah, A. B. Abdel-Rahman, and T. Sallam, "Performance improvement of high altitude platform using concentric circular antenna array based on particle swarm optimization," *AEU Int. J. Electron. Commun.*, vol. 91, pp. 85–90, 2018.

[16] X. Wu, B. Murherjee, and D. Ghosal, "Hierarchical architectures in the third-generation cellular network," *IEEE Wireless Commun.*, vol. 11, no. 3, pp. 62–71, 2004.

[17] S. Sekander, H. Tabassum, and E. Hossain, "Multi-tier drone architecture for 5G/B5G cellular networks: Challenges, trends, and prospects," *IEEE Commun. Mag.*, vol. 56, no. 3, pp. 96–103, 2018.

[18] S. C. Arum, D. Grace, P. D. Mitchell, M. D. Zakaria, and N. Morozs, "Energy Management of Solar-Powered Aircraft-Based High Altitude Platform for Wireless Communications," *MDPI Electron.*, vol. 9, no. 1, pp. 1–25, 2020.

[19] M. Helmy and H. Arslan, "Utilization of aerial heterogeneous cellular networks: Signal-to-interference ratio analysis," *J. Commun. Netw.*, vol. 20, no. 5, pp. 484–495, 2018.

[20] J. Qiu, D. Grace, G. Ding, M. D. Zakaria, and Q. Wu, "Air-Ground heterogeneous networks for 5G and beyond via integrating high and low altitude platforms," *IEEE Wireless Commun.*, vol. 26, no. 6, pp. 140–148, December 2019.

[21] T. Z. Oo et al., "Offloading in hetnet: A coordination of interference mitigation, user association, and resource allocation," *IEEE Trans. Mobile Comput.*, vol. 16, no. 8, pp. 2276–2291, 2017.

[22] X. Huang, W. Xu, G. Xie, S. Jin, and X. You, "Learning oriented cross-entropy approach to user association in load-balanced HetNet," *IEEE Wireless Commun. Lett.*, vol. 7, no. 6, pp. 1014–1017, 2018.

[23] A. Ghosh et al., "Heterogeneous cellular networks: From theory to practice," *IEEE Commun. Mag.*, vol. 50, no. 6, pp. 54–64, 2012.

[24] Cambridge Consultants, "The world's largest commercial airborne antenna," https://www.cambridgeconsultants.com/us/case-studies/worlds-largest-commercial-airborne-antenna, 2022, Accessed: 13-09-2022.

[25] P. Balling, "Multibeam antennas," *Encyclopedia RF Microwave Eng.*, 2005.

[26] W. Hong et al., "Multibeam antenna technologies for 5G wireless communications," *IEEE Trans. Antennas Propag.*, vol. 65, no. 12, pp. 6231–6249, 2017.

[27] H. Panfeng, C. Naiping, and N. Shuyan, "Coverage model of multi beam antenna from high altitude platform in the swing state," in *IEEE ICSESS*, 2016, pp. 750–753.

[28] Y. Xu, W. Zhu, J. Li, and L. Zhang, "Improvement of endurance performance for high-altitude solar-powered airships: A review," *Acta Astronautica*, vol. 167, pp. 245–259, 2020.

[29] H. Li, X. Xu, M. Yang, and Q. Guo, "Compensative mechanism based on steerable antennas for high altitude platform movement," in *EAI ChinaCom*, 2011, pp. 870–874.

[30] C. A. Balanis, *Antenna Theory: Analysis and Design*. John wiley & sons, 2016.

[31] Technical Specification Group, "GSM/EDGE; Radio Access Network; Radio transmission and reception," 3rd Generation Partnership Project (3GPP), Technical Specification TS 05.05, 11 2005, v8.20.0.

[32] Maxim Integrated Products Inc., "Introduction to GSM and GSM mobile RF transceiver derivation," https://www.maximintegrated.com/en/design/technical-documents/tutorials/2/2157.html, Sep. 2003, Accessed: 23-09-2022.

[33] J. Holis and P. Pechac, "Elevation dependent shadowing model for mobile communications via high altitude platforms in built-up areas," *IEEE Trans. Antennas Propag.*, vol. 56, no. 4, pp. 1078–1084, 2008.

[34] M. D. Zakaria, D. Grace, and P. D. Mitchell, "Antenna array beamforming strategies for high-altitude platform and terrestrial coexistence using K-means clustering," in *IEEE MICC*, Nov 2017, pp. 259–264.

[35] Technical Specification Group, "Radio Access Network; Study on New Radio (NR) to support non-terrestrial network," 3rd Generation Partnership Project (3GPP), Technical Report TR 38.811, 09 2020, v15.4.0.

[36] HAPS Alliance, "Bridging the digital divide with aviation in the stratosphere," https://hapsalliance.org/publications/, pp. 1–25, Dec. 2021, Accessed: 23-09-2022.

[37] Z. Lian, L. Jiang, C. He, and Q. Xi, "A novel channel model for 3-D HAP-MIMO communication systems," in *IEEE NaNA*, 2016, pp. 1–6.

[38] Z. Yang and A. Mohammed, "Deployment and capacity of mobile WiMAX from high altitude platform," in *IEEE VTC*, Sep. 2011, pp. 1–5.

[39] A. Burr, A. Papadogiannis, and T. Jiang, "MIMO truncated shannon bound for system level capacity evaluation of wireless networks," in *IEEE WCNCW*, April 2012, pp. 268–272.

[40] R. K. Jain, D.-M. W. Chiu, and W. R. Hawe, "A quantitative measure of fairness and discrimination," Eastern Research Laboratory, Digital Equipment Corporation, Hudson, MA, Tech. Rep. TR-301, Sep. 1984.

[41] M. C. Batistatos, G. V. Tsoulos, D. A. Zarbouti, G. E. Athanasiadou, and S. K. Goudos, "LTE measurements for flying relays," in *IEEE MOCAST*, 2018, pp. 1–4.

[42] M. Ndong and T. Fujii, "Cross-tier interference management with a distributed antenna system for multi-tier cellular networks," *EURASIP J. Wireless Commun. Netw.*, vol. 2014, no. 1, p. 73, 2014.

[43] M. Yassin et al., "Survey of ICIC techniques in LTE networks under various mobile environment parameters," *Springer Wireless Netw.*, vol. 23, no. 2, pp. 403–418, 2017.

David Grace (S'95-A'99-M'00-SM'13) received his PhD from University of York in 1999. Since 1994 he has been a member of the Department of Electronic Engineering at York, where he is now Professor (Research), Head of Communication Technologies Research Group, and Director of the Centre for High Altitude Platform Applications. Current research interests include aerial platform-based communications, application of artificial intelligence to wireless communications; 5G system architectures; dynamic spectrum access and interference management. He is currently a lead investigator on H2020 MCSA SPOTLIGHT, UK Government funded MANY, dealing with 5G trials in rural areas, and HiQ investigating Quantum Key Distribution from high altitude platforms. He was technical lead on the 14-partner FP6 CAPANINA project that dealt with broadband communications from high altitude platforms. He is an author of over 280 papers, and author/editor of 2 books. He is the former chair of IEEE Technical Committee on Cognitive Networks for the period 2013/4. He is a founding member of the IEEE Technical Committee on Green Communications and Computing. In 2000, he jointly founded SkyLARC Technologies Ltd, and was one of its directors.

Steve Chukwuebuka Arum received his B.Eng degree in Electronic Engineering from the University of Nigeria in 2012, as well as his M.Sc and Ph.D. degrees from the University of York UK in 2015 and 2022 respectively. Current research interests lie in aerial platform-based communication systems and networks, 5G and beyond system architecture, heterogeneous cellular network, and spectrum resource management. In 2017, He joined Huawei (Nig.) as an Assistant Product Engineer helping MNOs optimise their radio access network (RAN) and worked on projects including new 3G/4G base station build, radio resource unit modernisation, and cell multi-sectorisation. After his Ph.D on wireless coverage and capacity enhancement using high altitude platforms in 2021, he joined the wireless research team in the Applied Research and Network Strategy Department of BT where he is leading the non-terrestrial network research covering satellites and HAPs, and working on new RAN architectures including OpenRAN. Current projects include UK Government funded ARI-5G, which is looking to build and demonstrate a standards-based RIC platform with specific software solutions running on that platform, and the trial of HAP antenna array system for reconfigurable 5G coverage.

Paul D. Mitchell (M'00-SM'09) received the M.Eng. and Ph.D. degrees from the University of York in 1999 and 2003, respectively. He has over 20 years research experience in wireless communications, and industrial experience gained at BT and DERA (now QinetiQ). He has been a member of academic staff in the Department of Electronic Engineering at the University of York since 2005, and is now full Professor. Primary research interests lie in underwater acoustic communication networks, wireless sensor networks, high altitude platforms, satellite systems and communication protocols; including the development of novel medium access control and routing strategies. Other related interests include machine learning, traffic modelling, queuing theory, satellite and mobile communication systems. Professor Mitchell is an author of over 140 refereed journal and conference papers and he has served on numerous international conference programme committees including ICC and VTC. He was General Chair of the International Symposium on Wireless Communications Systems in 2010. He currently serves as an Associate Editor of the IET Wireless Sensor Systems journal, the International Journal of Distributed Sensor Networks and MDPI Electronics, and has experience as Guest Editor and as a reviewer for a number of IEEE, ACM and IET journals. He has secured more than £3.8M + €4.7M funding as principal and co-investigator. Current projects include Research Council grants on smart dust for large scale underwater wireless sensing, full-duplex underwater acoustic communications, as well as industrial projects. He is a Senior Member of the IEEE and a member of the IET.